Available online at www.sciencedirect.com
ScienceDirect
Materials and Design 28 (2007) 441–447
Materials & Design
www.elsevier.com/locate/matdes

Shape optimization of tooth profile of a flexspline for a harmonic drive by finite element modelling

Oguz Kayabasi *, Fehmi Erzincanli

Department of Design and Manufacturing Engineering, Gebze Institute of Technology, PK 141, Gebze, 41400 Kocaeli, Turkey

Received 21 April 2005; accepted 13 September 2005
Available online 26 October 2005

Abstract

Analytical procedures often fail to predict correctly the maximum stress and its position, a new, more reliable method is needed for that purpose. A computational stress–strain analysis of the flexible gear, based on the finite element method, is investigated as an alternative and is presented here. The aim of this study was to calculate the stress on flexspline teeth and find optimum shape of teeth to maximize fatigue life.

Finite element analysis of the harmonic drive flexspline shows that the numerical analysis provides better estimate of the maximum stress than the experimental procedures. This leads to the conclusion that only the proposed numerical procedure should be used when designing the flexspline. The presented approach to a stress-deformation analysis of the flexspline can help the designer to accurately determine the maximum stress on the flexspline, which can then be used for optimizations of the flexspline construction.

Keywords: Fatigue; Elastic behavior; Harmonic drive; Flexspline; Optimization

1. Introduction

Since 1965, when the American engineer Musser invented the first version of harmonic drive power transmission incorporating harmonic drive came to practical application [1–3]. Many researchers have conducted studies to improve performance since Musser had invented a harmonic drive [2–4]. Harmonic drive has several characteristic for instance, a high precision, compactness, light-in-weight property and high reduction ratio characteristics compared with the conventional speed reducer [5]. Harmonic gear drive is widely utilized in high performance control system. It is a very compact gear system, which is capable of producing speed ratios up to 300 in a single stage. Therefore, the harmonic drive is widely adopted in precision mechanism. The best known application of the harmonic drive is in industrial robots, where it is used as a device for reducing speed in the actuators, composed numerical control (CNC) machine tools and communication equipment.

The major benefits of harmonic drive systems are their superior weight to torque ratio, excellent angular positioning characteristics, essentially zero backlash and high, single-stage reduction ratios. The conventional speed reducer uses the concept of rigid bodies, but the harmonic drive is operated by the elastic theory. As for this, harmonic drive shows different characteristics in operation principles and analysis compared to the conventional ones. Harmonic gear drive consists of three components which called a rigid ''circular spline'', an elliptical ''wave generator'' and non-rigid ''flexspline''. Circular spline has an inner teeth and flexspline outer teeth. Wave generator has a ball bearing and it is elliptical shape. Its operation is based on a harmonic elastic deformation of the flexspline. Harmonic drive is shown in Fig. 1.

When the wave generator is rotated clockwise shown in Fig. 2(a) with the circular spline fixed, the flexspline is subjected to elastic deformation and its tooth engagement

* Corresponding author. Tel.: +90 262 653 8497; fax: +90 262 653 8490/0675.
E-mail address: oguzk@gyte.edu.tr (O. Kayabasi).

0261-3069/$ - see front matter © 2005 Elsevier Ltd. All rights reserved.
doi:10.1016/j.matdes.2005.09.009

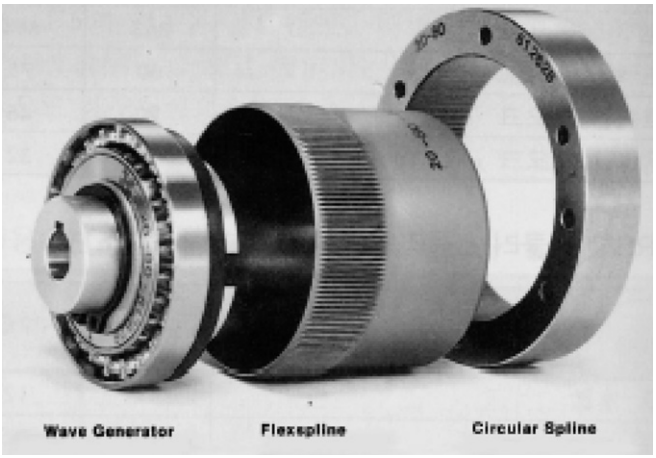

Fig. 1. Component of harmonic drive.

position moves by turns relative to the circular spline. When the wave generator rotates 180° clockwise shown in Fig. 2(b), the flexspline moves counterclockwise by one tooth relative to the circular spline. When the wave generator rotates one revolution clockwise shown in Fig. 2(c) (360°), the flexspline moves counterclockwise by two teeth relative to the circular spline because the flexspline has two fewer teeth than the circular spline. In general terms, this movement is treated as output power.

Analytical procedures often fail to predict correctly the maximum stress and its position, a new, more reliable method is needed for that purpose. A computational stress–strain analysis of the flexible gear, based on the finite element method (FEM), is investigated as an alternative and is presented here. The aim of this study was to calculate the stress on flexspline teeth and find optimum shape of teeth to maximize fatigue life. In this work, Pro/Engineer computer aided design (CAD) software package was used for design and ANSYS software for the finite element analysis (FEA). Many researcher have conducted studies to improve performance since Musser had invented a harmonic drive [3].

2. Experimental and analytical solutions

The flexspline tends to detach itself from the wave generator in the regions AB' and $A'B$ at some angle φ_M under the loading. After the major deformation axis due to circumferential buckling, this is illustrated on Fig. 3 with line 3. Line 1 represents the elliptical deformation shape of the flexspline caused by the inserted wave generator 2. Thin construction of the flexspline clearly offers very little resistance to the circumferential buckling.

The approximate loading conditions of the flexspline are shown in Fig. 4, where angles φ_1, φ_2 and φ_3 define the area of acting loads. Experimental measurements by Ivanov [7] showed that $\varphi_1 \approx -\pi/12$ and $\varphi_2 = \varphi_3 \approx \pi/8$. The distributed loads can in the case $\varphi_2 = \varphi_3$ be written in the interval $\langle \varphi_1 - \varphi_2, \varphi_1 + \varphi_2 \rangle$ as:

$$\begin{aligned} \bar{q}_\varphi &= \bar{q}_{\varphi\max} \cdot \cos[\pi \cdot (\varphi - \varphi_1)/(2\varphi_2)], \\ \bar{q}_r &= \bar{q}_\varphi \cdot \tan \alpha_{sr}, \end{aligned} \tag{1}$$

with

$$\bar{q}_{\varphi\max} = \frac{\pi \cdot T_2}{2\varphi_2 \cdot d_e^2 \cdot b_d}, \tag{2}$$

where T_2 is the output torque, d_e is the flexspline pitch diameter and b_d is the engagement width of the teeth.

The analytical procedure for determination of the stress-deformation state of the flexspline is based on the modified theory of shells, which is described by Ivanov [7] and summarized by Ren [6], and is due to its extensiveness not given

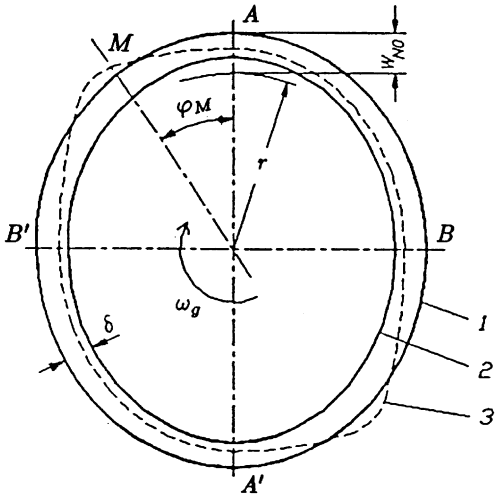

Fig. 3. The flexspline shape change under the loading.

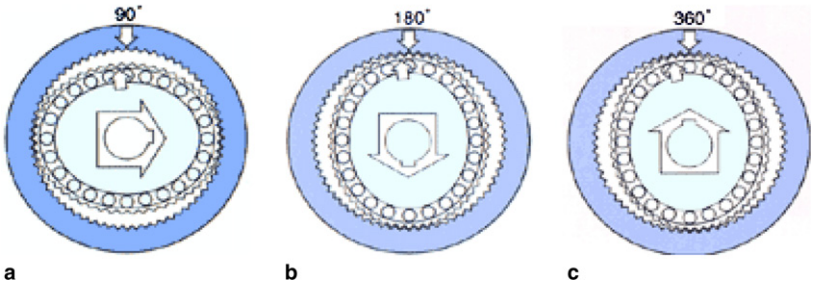

Fig. 2. Movements of harmonic drive.

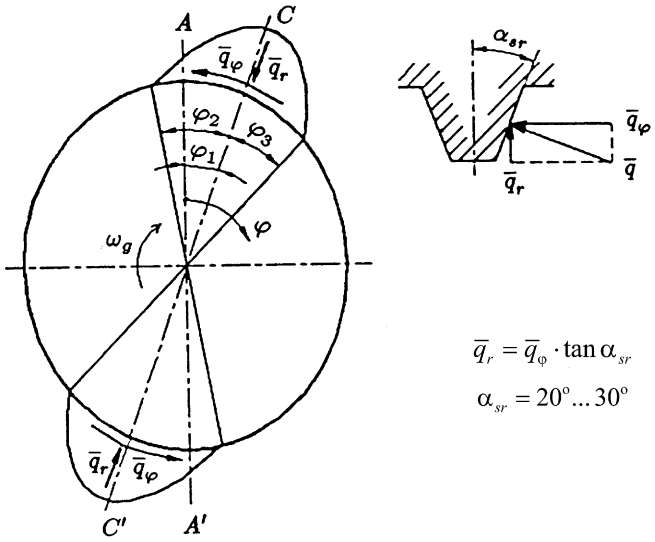

Fig. 4. The flexspline load distribution.

here. The analytical procedures assume that under the loading different regions of the flexspline deform in the shape of known geometrically curves, which are mathematically easy to describe. This gives raise to a discontinuous stress field along the circumference of the flexspline and overestimation of the peak stress, which is typically needed when designing the thickness of the flexspline. Therefore, a numerical analysis of the flexspline becomes a necessity for optimum design. In this study, harmonic drive prototype was manufactured to compare finite element results so experimental setup was set up. We propose a joint torque sensing technique using elasticity of the harmonic drive. The technique is based on the construction of the strain gauge bridges on the flexspline in harmonic drives, by which the modulation in the sensor output due to the wave generator rotation is eliminated. Following finite element modelling is explained.

3. Methods, geometric and finite element modeling

3.1. Methods

A shape or material design optimization problem can generally be formulated as a constrained minimization problem as following:

minimize :

$$y_0(\mathbf{x}) \tag{3}$$

subjected to :

$$y_j(\mathbf{x}) \leqslant 0 \quad (j = 1, \ldots, n_c) \tag{4}$$

within the design space :

$$x_{il} \leqslant x_i \leqslant x_{iu} \quad (i = 1, \ldots, N), \tag{5}$$

where $y_0(\mathbf{x})$ is the objective function, $y_j(\mathbf{x})$ $(j = 1,\ldots,n_c)$ are the constraint functions and $\mathbf{x} = [x_1,x_2,\ldots,x_N]$ is the vector of design variables. x_{il} and x_{iu} describe physical upper and lower bounds on design variables. n_c and N are the number of constraints and number of design variables, respectively. The constraint and objective functions may correspond to weight, penetration depth, energy absorption, etc.

Solution of Eqs. (3) and (4) for shape optimization problems can be efficiently done by replacing objective and constraint functions with their response surface (RS) approximations. Optimization with approximations is often referred to as approximate optimization in the literature. The approximate optimization method implemented in ANSYS DO module and used in this paper is shown in Fig. 5. ANSYS DO module generates and utilizes polynomial RS approximation for objective or constraint function as following [1]:

$$\tilde{y}(\mathbf{x}) = \underbrace{a_0 + \sum_{n=1}^{N} a_n x_{n\,\text{linear}}}_{} + \underbrace{\sum_{n=1}^{N} b_n x^2_{n\,\text{quadratic}}}_{} + \underbrace{\sum_{m=1}^{N-1} \sum_{n=m+1}^{N} c_{mn} x_m x_{n\,\text{quadratic+crossterms}}}_{}, \tag{6}$$

where a, b, c are coefficients to be determined.

In design optimization process, ANSYS DO first creates $N+2$ design sets to construct a linear approximation. Here, set indicates values of all parameters for a specific design. ANSYS DO will either generate design sets randomly or use the existing ones in the optimization database. Shape optimization analysis is carried out at available design sets. Analysis results are then used to create linear approximations of objective and constraints. Higher order approximations such as quadratic and quadratic with cross terms RS approximations are created using least square method when there are enough design sets in the database. The optimum design is predicted by solving Eqs. (3)–(5) with a numerical optimization algorithm based on penalty functions. The predicted optimum is verified by exact analysis (ANSYS). If the predicted objective and constraints are identical with the results from ANSYS, or the estimated optimum design is satisfactory enough, the optimization loop is stopped. Otherwise, the newly calculated results

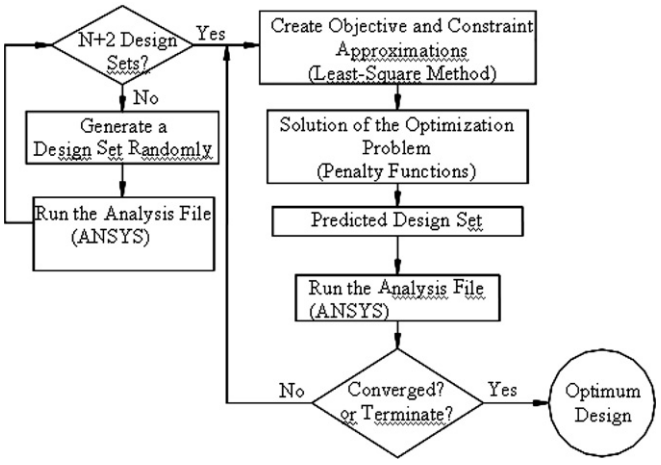

Fig. 5. Approximate design optimization process with ANSYS DO module.

are added to the existing design sets and new approximations are created followed by the solution of the optimization problem.

3.2. Geometric modelling

In general harmonic gear drive consists of three components which called a rigid "circular spline", an elliptical "wave generator" and nonrigid "flexspline". Circular spline has an inner teeth and flexspline outer teeth. Wave generator has a ball bearing and it is elliptical shape. When wave generator is inserted into flexspline flexspline is shaped as an elliptical, so flexspline was modeled elliptical shape for finite element analysis. Wave generator has a ball bearing and it is elliptical shape. Modeled ball bearing is not necessary for finite element analysis because of calculation time, so wave generator was modeled elliptical rigid shape. Flexspline was modeled as shown in Fig. 6.

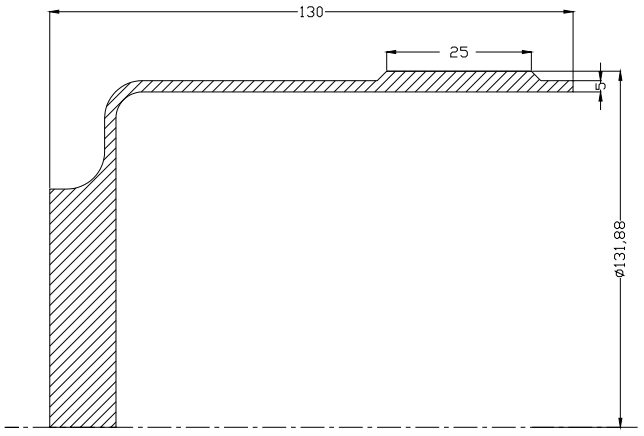

Fig. 6. Flexspline cross-section.

Design of the teeth profile of flexspline is of interest to reduce stress on teeth and increase fatigue life. The goal and the requirements are expressed in the form of an optimization problem as following:

find :

$$\mathbf{x} = \{N, \alpha_{sr}, \bar{q}\} \tag{7}$$

to minimize :

$$(\sigma, \text{displacement}) \tag{8}$$

subjected to :

$$\left.\begin{array}{l} 1.5 \leqslant N \leqslant 3 \\ 20\ \text{MPa} \leqslant \bar{q} \leqslant 250\ \text{MPa} \\ 20^\circ \leqslant \alpha_{sr} \leqslant 45^\circ, \end{array}\right\} \tag{9}$$

where N is the safety factor. α_{sr} is the pressure angle $\bar{q}$. Initial values of design parameters were taken as $N = 1.5$, $\alpha_s = 20^\circ$, $\alpha = 5^\circ$.

3.3. Finite element modeling

The first step with finite element method in numeric solution is to build finite element model equivalent to geometric model. Shell element can not consider thickness direction in joint parts, and cannot make a modeling with external gear. Though flexspline is a thin shell type, three-dimensional elements have to be used [5,8]. In this work, circular spline and flexspline were meshed using 8 node hexagonal elements. Mesh density is gradually coarsening from loading surface, which is potential contact region, to teeth. The complete model consisted of 12,840 elements. The circular spline consisted of 4560 elements, the flexspline consisted of 8280 elements. The circular spline and the flexspline were modeled with SOLID45 which is element type library of ANSYS, defined by 8 nodes each having three degree of freedom. Finite element modeling of flexspline is shown in Fig. 7.

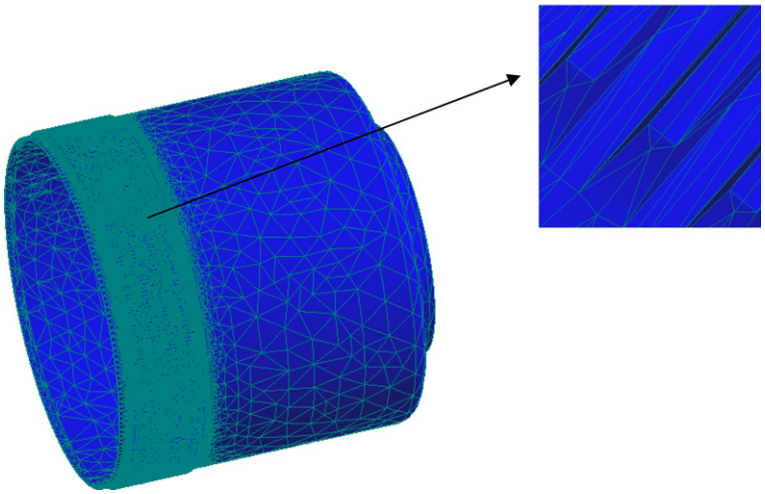

Fig. 7. Finite element model of flexspline.

Physical interactions among teeth, which were involved in the analysis, were simulated by using contact elements. The outer ring was modeled rigid as in the ideal wave generator. The stiffness of each roller represented by a single contact element CONTA26. For these elements a low stiffness constant $k_w = F/\delta = 3.6.10^4$ N/mm, corresponding to a low contact force F, was chosen, in order to obtain most accurate results nearby zero load. This selection is treated more thoroughly in the next section.

The second step of finite element method is to select material models which represent behavior of materials. For circular spline and flexspline material properties were used as shown Table 1.

The alternating stress versus number of cycles (S–N curve) for flexspline material used in this study for fatigue calculations was given in logarithmic scale in Fig. 8.

A good gear system design should satisfy maximum or an infinite fatigue life and reduce fatigue effects on teeth profile. This can only be ensured by physical testing or a fatigue analysis. In this study, fatigue life of the prosthesis upon finite element stress analysis is predicted using the computer code of ANSYS/Workbench [9]. Fatigue life of prosthesis is calculated based on Goodman, Soderberg and Gerber fatigue theories which are illustrated in Table 2.

Table 1
Properties of the steel 42CrMo4

Tensile modulus (GPa)	210
Shear modulus (GPa)	80
Poisson's ratio	0.3
Tensile strength (MPa)	1000
Density (kg/m^3)	7850

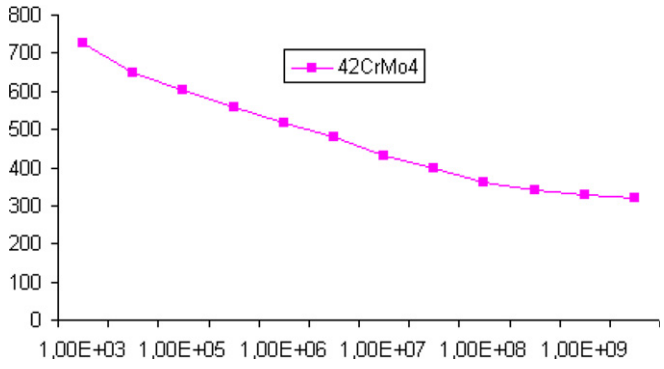

Fig. 8. Fatigue curves (S–N Curve) for 42CrMo4 material.

Table 2
Fatigue theories and formulas used in fatigue life predictions

Fatigue theories	Fatigue formulas
Goodman	$\left(\frac{\sigma_a}{S_e}\right) + \left(\frac{\sigma_m}{S_u}\right) = \frac{1}{N}$
Soderberg	$\left(\frac{\sigma_a}{S_e}\right) + \left(\frac{\sigma_m}{S_y}\right) = \frac{1}{N}$
Gerber	$\left(\frac{N\sigma_a}{S_e}\right) + \left(\frac{N\sigma_m}{S_u}\right)^2 = 1$

In Table 2, N indicates safety factor for fatigue life in loading cycle, S_e for endurance limit and S_u for ultimate tensile strength of the material. Mean stress σ_m and alternating stress σ_a are defined, respectively, as:

$$\sigma_m = \frac{(\sigma_{max} + \sigma_{min})}{2}, \tag{10}$$

$$\sigma_a = \frac{(\sigma_{max} - \sigma_{min})}{2}. \tag{11}$$

Von Misses stresses obtained from finite element analyses are utilized in fatigue life calculations. All fatigue analyses are performed according to infinite life criteria (i.e. $N = 10^9$ cycles).

The third step of finite element method is to apply loading and boundary condition. In all load steps the flexspline was supported in the plane $y = 0$. The wave generation was implemented in the first three load steps. The flexspline had temporary supports in the tangential direction in the planes $x = 0$ and $y = 0$. Because the continuously meshing teeth have no allowance, the teeth of outer and inner gears were displaced radially away from the flexspline to give space for the wave generation. Torque loading was implemented by rigid body rotation of the inner gear, which was the secondary or output member of the drive. The rigid outer gear was fixed, and the wave generator had its tangential supports in the plane $x = 0$. The same values of secondary torsion were given to the model. Secondary torque achieved depended on the stiffness of the drive. Secondary torsion $\zeta = 0.00125$ was well within the normal working range, so it was chosen as the reference point for torque comparisons.

During the simulation process, all input data was prepared using implicit non-linear finite element software ANSYS pre-processor and post-processor. The complete analysis and post-processing was performed on a P4 2 GHz Intel processor and 1 GHz RDRAM computer running Windows 2000. Displacement and bending stress were calculated. Analyses took about 13 h of CPU time

4. Results and discussion

As the deformation of a flexspline caused by the inserted wave generator is symmetrical around both elliptical deformation axes, only a quarter of the flexspline can be considered with prescribed double symmetry conditions. The wave generator construction used in the designed harmonic drive is that of a two, eccentrically and opposite positioned discs, where the contact between the flexspline and each of the discs is achieved along the angle $\pm\gamma = 30°$ measured from the major symmetrical axis. The radial displacements of the flexspline along this angle are therefore known and are prescribed to the inner nodes of the discretized model. Fig. 9 shows the computed circumferential displacements and Fig. 10 the maximum circumferential bending stress at the outer face of the flexspline. It can be seen, that numerical results coincide well with the experimental results.

The radial displacements of the inner boundary of the flexspline, obtained from the nonlinear contact analysis,

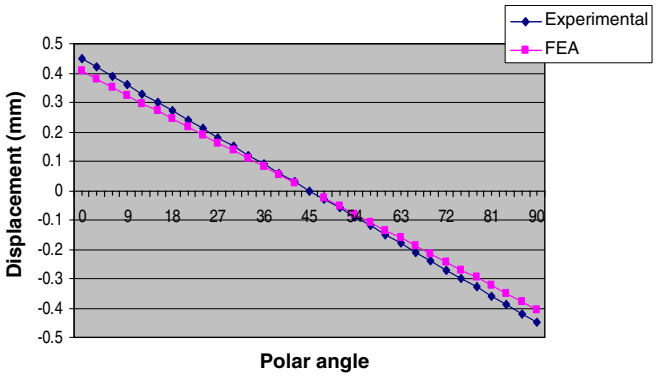

Fig. 9. Displacement of the flexspline due to insertion of the wave generator.

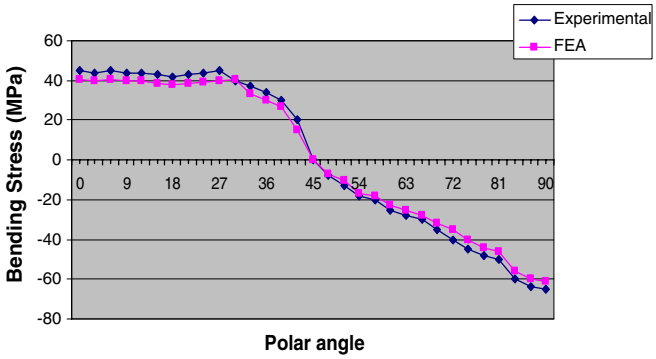

Fig. 10. Bending stresses of the deformed flexspline.

are shown in Fig. 11 with the solid line, where $\varphi = 0°$ corresponds to the major deformation axis. The radial displacements of the flexspline due to the wave generator are represented with the dotted line. It can be seen, that the experimentally observed detachment of a loaded flexspline from the wave generator, just after the main deformation axis, is also evident in the numerical analysis. The circumferential buckling in the region $-60° < \varphi < 0°$ is clearly observed.

The goal of this part of study was to find a drive having largest possible stiffness, in Fig. 12. shown that three shape of flexspline teeth profile changing iteration. Best results give in (a) shape profile. This results are shown in Fig. 13. As seen from the given table minimum von Mises stress occurred on shape (a). Maximum stress occurred on shape (c).

Prior to the fatigue analysis von Mises stresses obtained due to the applied loads were compared with the previous works to validate the model and to ensure the model safety against static failure.

Goodman, Soderberg and Gerber were used for the fatigue analysis. Equivalent (von Mises) alternating stress and safety factor values were obtained for each option, geometry type and material property. All the analysis were performed according to infinite life criteria (1e9 cycles). It is important that these maximum equivalent stress values should be lower than the endurance limit of the material. The endurance limit of 41CrMo4 is 375 MPa. A minimum

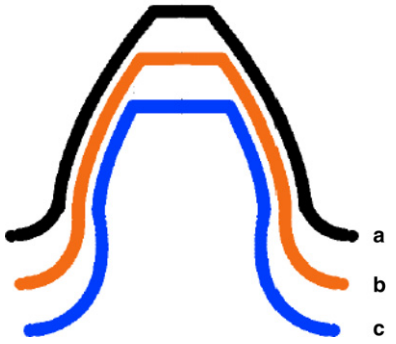

Fig. 12. Teeth profile while changing iteration.

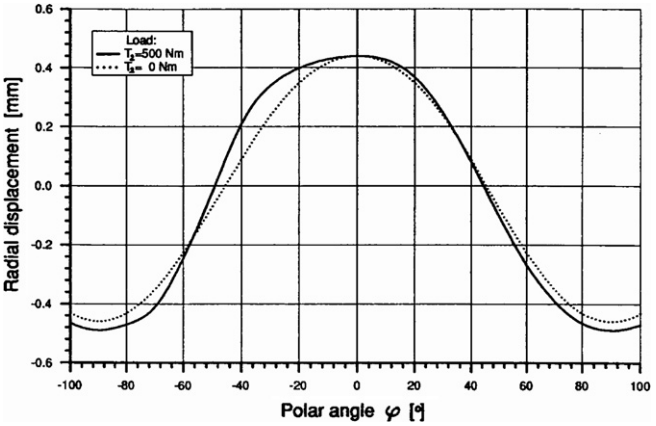

Fig. 11. Radial displacements of the loaded flexspline.

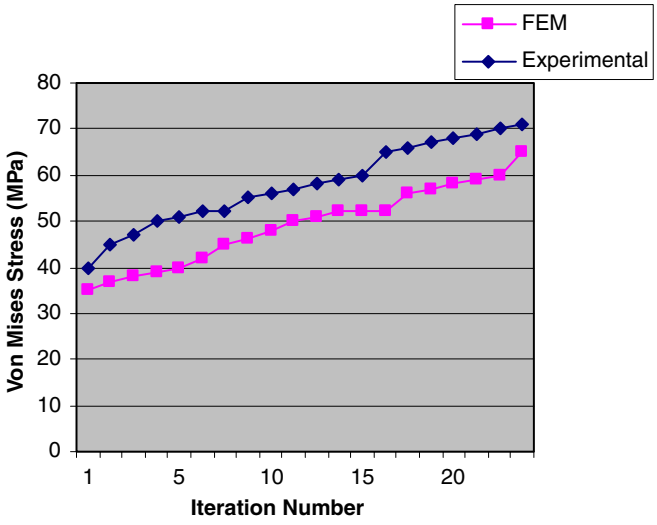

Fig. 13. Von Mises stress.

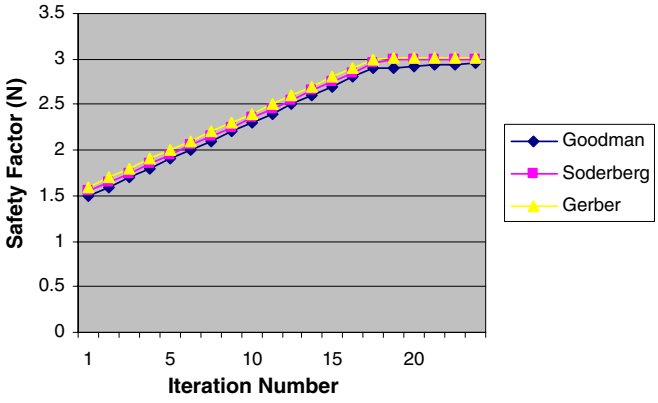

Fig. 14. Safety factor.

safety factor value for 42CrMo4 is given in Fig. 14. As seen from the obtained data Gerber theory gives the most conservative results and mean stress curve option results the highest safety factor values.

5. Conclusions

Finite Element Analysis of the harmonic drive flexspline shows that the numerical analysis provides better estimate of the maximum stress than the experimental procedures. This leads to the conclusion that only the proposed numerical procedure should be used when designing the flexspline. The presented approach to a stress-deformation analysis of the flexspline can help the designer to accurately determine the maximum stress on the flexspline, which can then be used for optimizations of the flexspline construction.

References

[1] Musser CW. Gear mechanism, US Patent No. 3 178 963, 20 April 1965.
[2] Tutle TD. Understanding and modelling the behavior of a harmonic drive gear transmission, MIT Technical Report 1365, MIT Artificial Intelligence Laboratory; 1992.
[3] Vladis K. Analytical investigation of the change in phase angle between the wave generator and the teeth meshing zone in high-torque mechanical harmonic drives. Mech Mach Theory 1997;32(5):533–8.
[4] Kiyosawa Y, Takizawa N, Ohkura T, Yamamoto Y. A new strain wave gearing. JSME 23–26 November 1991: p. 1132–6.
[5] Jeon Han Su, Oh Se Hoon. A study on stress and vibration analysis of a steel and hybrid flexspline for harmonic drive. Compos Struct 1997;47:827–33.
[6] Ren Z. The design and construction of the harmonic drive and stress analysis of its flexible element, M.Sc. Thesis, University of Maribor, 1990.
[7] Ivanov MN. Harmonic gear drives. Višaja škola, Moscow, 1981.
[8] Oh Se Hoon, Chang Seung Hwan, Lee Dai Gil. Improvement of the dynamic properties of the steel-composite hybrid flexspline for a harmonic drive. Compos Struct 1997;38(1–4):251–60.
[9] ANSYS 9.0. User Manual.